ELSEVIER

Biophysical Chemistry 103 (2003) 99–107

Biophysical Chemistry

www.elsevier.com/locate/bpc

Ferricytochrome *c* encapsulated in silica hydrogels: correlation between active site dynamics and solvent structure

Maria Grazia Santangelo, Matteo Levantino, Eugenio Vitrano, Antonio Cupane*

National Institute for the Physics of Matter (INFM) and Department of Physical and Astronomical Sciences (DSFA), University of Palermo, via Archirafi 36, I-90123 Palermo, Italy

Received 27 May 2002; received in revised form 15 July 2002; accepted 15 July 2002

Abstract

Ferricytochrome *c* encapsulated in silica hydrogels has been prepared by the sol–gel technique following, with some modifications, the procedure originally developed by Zink et al. A suitable preparation of hydrogels enables to have both 'wet' and 'dry' samples. Wet samples have a high water content: as the temperature is lowered below ~260 K water freezes and the samples crack. On the contrary, dry samples have a low water content (hydration $h \sim 0.35$): in these conditions water does not freeze even at cryogenic temperatures and the samples remain transparent and non-cracking. The dynamics of ferricytochrome *c* and its dependence on the surrounding medium have been studied by optical absorption spectroscopy in the temperature range 10–300 K. At each temperature, spectra were collected both in the Soret region and in the near infrared at ~1.45 μm (the water overtone band); this enables to probe the local dynamics of the protein active site as well as the 'structure' of water molecules present in the sample. The data show that sol–gel encapsulation 'per se' does not alter the protein active site dynamics, but rather introduces an increased local heterogeneity. At difference, we find a correlation between active site dynamics and water structure: in the wet hydrogel, freezing of water quenches the ensemble of soft modes linearly coupled to the Soret transition; while, in the dry hydrogel, water does not freeze, and an active site dynamic behavior—similar to the non-freezing water/glycerol solution—is observed.

Keywords: Sol–gel encapsulation; Protein dynamics; Optical absorption spectroscopy

1. Introduction

Encapsulation of proteins in porous silica hydrogels derived from tetramethylorthosilicate (TMOS) through the sol–gel technique is being widely used in both biotechnology and basic research. In fact, encapsulated proteins show enhanced stability while retaining almost completely their functional and spectral properties [1–4], and are thus good candidates for use as biosensors and optical gas sensors [5]. From the point of view of fundamental research, it has been shown that sol–gel encapsulation sizably limits the degree of conformational freedom of proteins and slows the kinetics of conformational changes. The sol–gel technique

*Corresponding author. Tel.: +39-916234221; fax: +39-916162461.

E-mail address: cupane@fisica.unipa.it (A. Cupane).

0301-4622/03/$ - see front matter © 2002 Elsevier Science B.V. All rights reserved.
PII: S0301-4622(02)00246-6

has therefore been used to block the T ⇔ R quaternary transition of hemoglobin, and to study the equilibrium and the kinetics of ligand binding to this protein in a given quaternary conformation [6–10]. The unfolding and refolding of encapsulated myoglobin has also been studied using several optical techniques together with different unfolding/refolding protocols [11].

On the other hand, proteins are widely recognized as dynamic entities characterized by a largely degenerate ground state and therefore fluctuating, at room temperature, among a large subset of conformational substates [12]. Protein equilibrium fluctuations have also been shown to have a relevant role in determining protein functionality [13–16]. Studies on protein dynamics are therefore necessary to obtain a deeper understanding on protein stability and function; dynamics studies of encapsulated proteins however, although highly desirable, are at present lacking.

It is now widely accepted that the local equilibrium dynamics of the active site of metalloproteins can be studied through the temperature dependence of the optical spectra. In fact, it has been shown that analysis of the thermal behavior of the Soret band line-shape of heme-proteins gives information on the ensemble of low-frequency vibrational modes that are coupled to the electronic transition responsible for the Soret band. Since this transition is localized at the heme, but greatly influenced by the surrounding environment, this analysis gives information on the local dynamic properties of the heme/heme-pocket/solvent system [17–20]. However, the above approach requires to have samples that remain homogeneous and transparent down to cryogenic temperatures and therefore, the studies referred to above were performed using water/cryoprotectant (usually glycerol) solutions.

Recently, we have developed a sol–gel protocol that enables to have samples of vitreous transparent material which, after suitable aging, remain homogeneous and transparent even at 5 K, thus allowing to perform optical absorption measurements down to cryogenic temperatures. In a previous work [21], we have exploited this new protocol to study the temperature dependence of the NIR absorption bands of water trapped in our silica hydrogels and to obtain information on its structural properties.

In this work, we report the temperature dependence of the Soret band of ferricytochrome *c* encapsulated in silica hydrogels of different aging periods, in comparison with the behavior in water and water/glycerol solutions. In the same hydrogels, we measure also the temperature dependence of the NIR absorption bands of water trapped in the silica matrix.

The purpose of the work is twofold:

- to characterize the active site dynamics of the sol–gel encapsulated protein, also in connection with the aging of the gel;
- to exploit the possibility of measuring, in the same sample, the Soret band and the water near infrared spectra in order to study the relation of protein active site dynamics with the structure of water trapped in the hydrogel.

2. Materials and methods

2.1. Samples preparation

Horse heart ferricytochrome *c* was purchased from Sigma and used without further purification. The cytochrome *c* 'solution samples' were prepared by diluting a concentrated protein stock solution into the appropriate water–glycerol-buffer solutions, in order to obtain a final protein concentration of approximately 8 μM in 0.1 M phosphate buffer at pH 5. Our sample in glycerol/water solution is different from that used in the work by Militello et al. (2002) [22] since, we use 65% v/v glycerol/water at pH 5 instead of 70% v/v glycerol/water at pH 7. Use of a buffer at pH 5 is due to the fact that the pH of the sol–gel encapsulated samples is approximately 5, as measured in the sol before gelification. The sol–gel encapsulated cytochrome *c* samples were prepared by mixing, in a 1:1 proportion, a cytochrome *c* solution ($\sim$20 μM in 0.1 M phosphate buffer pH 7) with a mixture of 75% TMOS (Sigma), 23% deionized Millipore water and 2% HCl 0.05 M previously sonicated for 20 min in an ice bath. After mixing, the resulting sol (pH $\approx$ 5) was poured

into semi-micro methacrylate cuvettes (Kartell, 1 cm path length) and, within some minutes, the gel was formed. After approximately 1 day the gel (a $3.1\times1.0\times0.44$ cm^3 slab of vitreous transparent material) was taken out from the cuvette. We call this sample 'wet hydrogel'. A wet hydrogel sample was left to age for several months. During the aging process the gel lost water and contracted. The 5 month aged sample—which we call 'dry hydrogel'—had final dimensions of approximately $1.7\times0.5\times0.24$ cm^3 and hydration level (grams H_2O/grams SiO_2) $h=0.35$. All steps of gel preparation, including aging, were performed at 7 °C in the cold room.

2.2. Absorption measurements

Absorption spectra in the range 350–480 nm and 1.2–1.8 μm were measured with a Jasco V-570 spectrophotometer. The experimental conditions were as follows: scan speed = 0.33 nm s^{-1} (Visible) or 1.66 nm s^{-1} (NIR), integration time = 1 s, bandwidth = 0.5 nm (Visible) or 2 nm (NIR), corresponding to a spectral resolution of ~30 cm^{-1} at 400 nm and ~10 cm^{-1} at 1.45 μm. Measured spectra were digitized at 0.5 nm intervals in the visible region, and at 1.0 nm intervals in the near infrared region.

Samples were put on the suitably modified copper sample holder of an Oxford Instruments (Aldington, UK) Optistat cryostat. The temperature was measured in the copper sample holder and was controlled to within ±0.5 K with an Oxford Instruments ITC 503 temperature controller. The cooling rate was approximately 1 K min^{-1}; at each temperature, the sample was left to equilibrate for at least 15 min prior to the spectral measurement. Repeated scans at selected temperatures gave indistinguishable results, thus confirming the full thermal equilibration of the sample. Hysteresis upon temperature cycling was not observed.

2.3. Spectral analysis

The procedure adopted to analyze the Soret band profiles at various temperatures has been reported in previous publications [18,22] and only the principal aspects of the analysis are given here. The absorption line-shape of the Soret band results from a Franck-Condon type coupling of a fully allowed electronic transition of the porphyrin (from the ground to the so-called B excited state) with vibrational modes of the system. Under this hypothesis the spectral profile can be described by the convolution of two terms:

$$A(\nu)=M^2\nu[L(\nu)\otimes G(\nu)] \tag{1}$$

where M is a constant proportional to the matrix element of the electric dipole moment. The ⊗ symbol stands for the convolution operation. The first term of the convolution, $L(\nu)$, is a Lorentzian line-shape that takes into account the coupling between the electronic transition and the high frequency modes of the system (defined as normal modes whose vibrational energy is larger than the thermal energy in the whole temperature range investigated, i.e. $h\nu \gg kT$). In the framework of Franck-Condon approximation $L(\nu)$ can be written as:

$$L(\nu)=\sum_{m_1\ldots m_h}^{\infty}\left[\prod_h^{N_h}\frac{S_h^{m_h}\mathrm{e}^{-S_h}}{m_h!}\right]\frac{\Gamma}{\left[\nu-\nu_0(T)-\sum_h^{N_h}m_h\nu_h\right]^2+\Gamma^2} \tag{2}$$

where: N_h is the number of high frequency modes vibronically coupled to the electronic transition; S_h is the linear coupling constant between the electronic transition and the h-th high frequency (ν_h) normal mode; ν_0 is the frequency of the purely electronic transition; Γ is the homogeneous (Lorentzian) width of the band.

In analogy with the work by Militello et al. [22], only the high frequency vibrational modes at $\nu_1=681$ cm^{-1} and $\nu_2=1372$ cm^{-1} were considered in the fitting procedure. These are the most coupled vibrational modes to the electronic transition as determined by resonance Raman spectroscopy [23,24]. Indeed, coupling with the modes at 1503, 1583 and 1636 cm^{-1} is not detected with our technique [22]; moreover, in view of the rather large Γ values, we are not able to resolve any coupling to the vibrational modes detected by

resonance Raman spectroscopy in the range 350–550 cm^{-1}. The S_{1372} values were found to be temperature independent; a ~20% increase of S_{681} was present at high temperatures.

The second term, $G(\nu)$, describes the coupling of the electronic transition with a bath of soft modes ($h\nu$ of the same order of or smaller than kT). It can be shown that $G(\nu)$, in the so-called 'short times approximation' [25,26] is a Gaussian:

$$G(\nu)=\frac{1}{\sigma(T)(2\pi)^{1/2}}\exp\left(-\nu^2/2\sigma^2(T)\right) \quad (3)$$

Using the harmonic Einstein approximation for the bath of low-frequency modes, the temperature dependence of Gaussian width is given by:

$$\sigma^2(T)=NS\langle\nu\rangle^2\coth\left(\frac{h\langle\nu\rangle}{2kT}\right)+\sigma^2_{\text{inh}} \quad (4)$$

where N, S, $\langle\nu\rangle$ are, respectively, the total number, the effective linear coupling constant and the frequency of the Einstein oscillator representing the soft modes bath. In Eq. (4), σ_{inh} accounts for the temperature independent inhomogeneous broadening.

3. Results and discussion

The Soret spectra at various temperatures measured with our 'solution samples' are very similar to those reported by Militello et al. [22] and are therefore not shown in this work.

Fig. 1a reports the Soret spectra of ferricytochrome *c* encapsulated in a wet hydrogel, measured at selected temperatures. The NIR spectra of water trapped in the same hydrogel are reported in Fig. 1b. Between 265 and 250 K the water in the wet hydrogel freezes and the sample cracks. This is clearly shown by the baseline increase of approximately 1.2 absorbance units, due to scattering, and by the appearance of a NIR spectrum typical of ice [27] (Fig. 1b). Due to excessive noise and spectral distortions arising from the large absorption, it is not possible to analyze quantitatively the water NIR spectra in Fig. 3b. We note, however, that the band at 1.39 μm—typical of Si–OH groups [28]—is not detected, and that the crystallized sample does not exhibit any absorption at

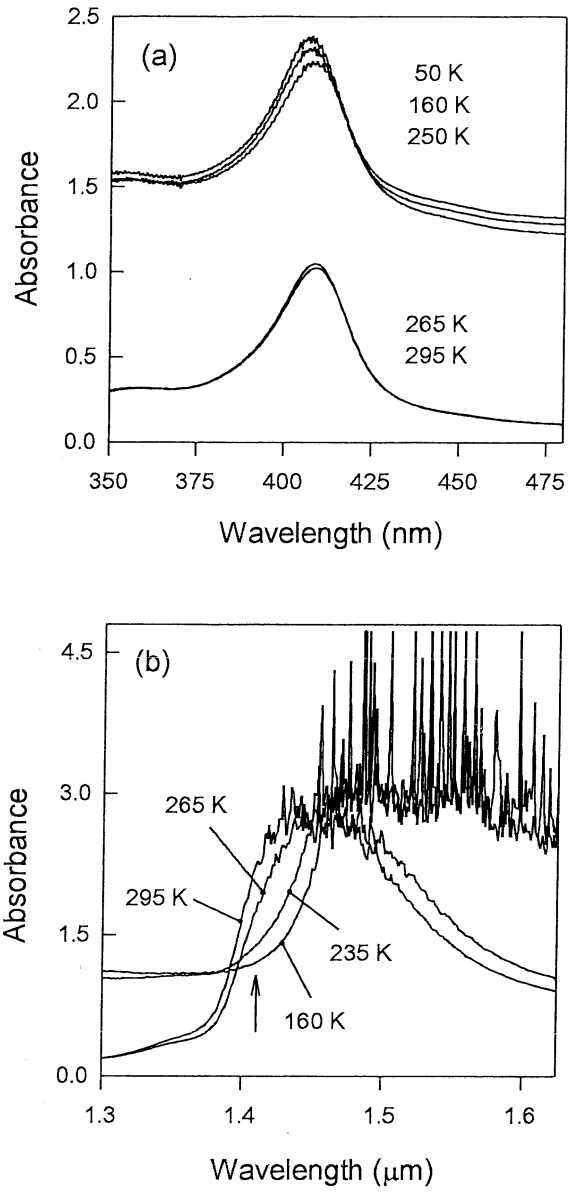

Fig. 1. (a) Soret band of encapsulated ferricytochrome *c* (wet hydrogel) at selected temperatures. (b) Near infrared absorption spectra (~1.45 μm overtone band) of water trapped in the wet silica hydrogel at selected temperatures. The arrow indicates the wavelength of 1.411 μm, where 'weakly bonded' water molecules absorb.

1.41 μm (see the arrow in Fig. 1b), where 'weakly bonded' water molecules are reported to absorb [27,29]. At difference, Fig. 1a shows that, despite

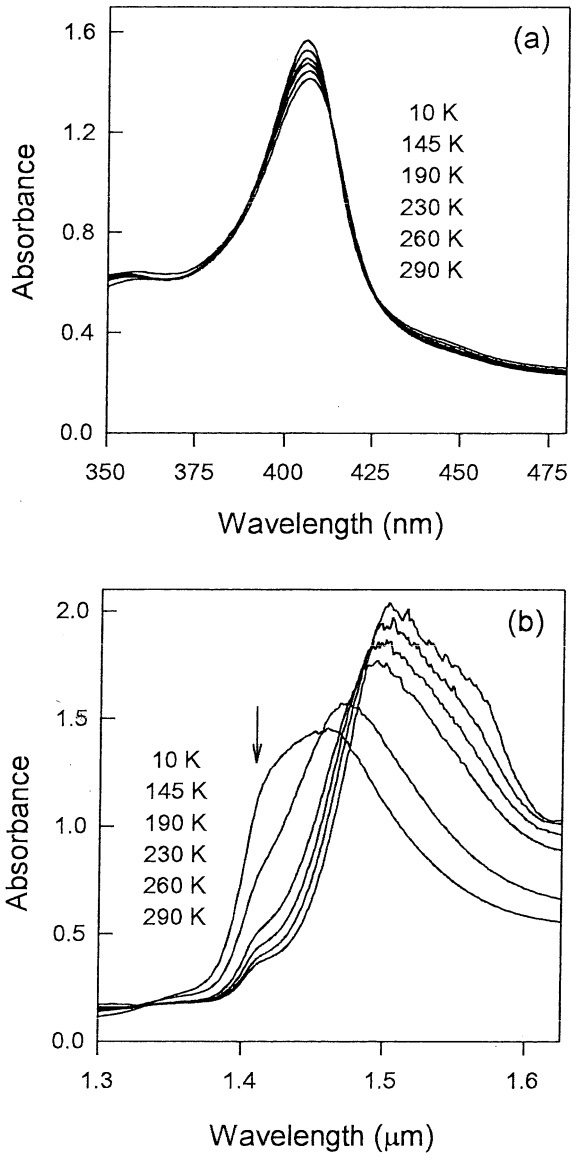

Fig. 2. Same as Fig. 1, for the 'dry' hydrogel.

the baseline jump and increased noise, it is still possible to measure the Soret band of cytochrome *c* encapsulated in the wet hydrogel down to cryogenic temperatures. This implies that it is possible to follow the protein active site dynamics in a completely frozen matrix.

Fig. 2a reports the Soret spectra of ferricytochrome *c* encapsulated in a 'dry' hydrogel (aging time ~5 months), measured at selected temperatures in the range 290–10 K; the NIR spectra of water trapped in the same hydrogel are reported in Fig. 2b. In the dry hydrogel, no water freezing and sample cracking occurs in the whole temperature range investigated: the dry hydrogel remains homogeneous and transparent down to 10 K and no baseline increase due to scattering is observed, both in the NIR and Soret spectral regions.

As the temperature is lowered, the NIR spectra of water trapped in the dry hydrogel monotonously move toward an 'ice-like' spectrum, with, however, one relevant difference: in fact, the absorption band at ~1.41 μm—which is characteristic of 'weakly bonded' water molecules, and is totally absent in the low temperature spectra of the cracked wet hydrogel (Fig. 1b)—is detected at all temperatures, even at 10 K.

A more quantitative analysis of the NIR spectra of water trapped in wet and dry silica hydrogels, has been reported in a previous work of our group [21]. Independent on any quantitative analysis, however, the spectra in Fig. 2b show that in the dry hydrogel the constraints imposed by the silica matrix on the trapped water molecules are such to prevent the formation of an extended ice-like structure and crystallization of the sample. Analysis of the temperature dependence of the Soret spectra shown in Fig. 2a therefore allows to investigate the active site dynamics of the protein in a non-frozen matrix in which a small percentage of 'weakly bonded' water molecules is still present even at 10 K.

Fig. 3 shows the deconvolution of the Soret spectra of ferricytochrome *c* encapsulated in the 'dry' silica hydrogel in terms of Eqs. (1)–(3). The deconvolution is similar to that used by Militello et al. [22], and includes two Gaussian components, centered at 2.29 and 2.76 μm^{-1}, that take into account spectral contributions of the N band and of the shoulder on the red side of the spectra. As shown in Fig. 3, the quality of the fit is excellent, as demonstrated also by the residuals, reported in the upper panel; fittings of analogous (or better), quality are obtained for each temperature. Values of the homogeneous width (parameter Γ) and of the coupling constants to the high frequency modes (parameters S_h) are reported in Table 1. Data in

Table 1 show that gel encapsulation does not introduce relevant alterations on these 'structural' parameters (except for an increase of the S_{681} value in the dry hydrogel), suggesting that the local porphyrin structure is very similar in the three samples.

Fig. 4 reports the temperature dependence of the squared Gaussian width (parameter σ^2) of the Soret band of ferricytochrome *c* encapsulated in a 'wet' and in a 'dry' silica hydrogel; data relative to ferricytochrome *c* in solution (both water and water/glycerol) are also reported for comparison.

The results relative to solution samples are in agreement with previous data of Militello et al. [22] in that they show that active site dynamics of ferricytochrome *c* (as monitored by the Gaussian broadening of the Soret band) follows, in the entire temperature interval 10–300 K, an harmonic behavior (Eq. (4) in Section 2). The σ^2 thermal behavior of the 'dry' sample is similar to that of the solution: a monotonous σ^2 decrease is observed upon lowering temperature and the data are in good agreement with the predictions of the harmonic Einstein approximation in the whole temperature range investigated. Parameters obtained by fitting the solution and 'dry' hydrogel data in terms of Eq. (4) are reported in Table 2; they show that, while the values of the average frequency of the soft modes and of the average linear coupling constant to the low-frequency bath are

Table 1
Values of the homogeneous width (Γ) and linear coupling constant (S_h) obtained from the analysis of the Soret band in terms of Eqs. (1)–(3)

Conditions	Γ (cm^{-1})	S_{681}	S_{1372}
Solution	500 ± 20	0.15 ± 0.05	0.1 ± 0.03
Wet hydrogel	500 ± 20	0.18 ± 0.05	0.1 ± 0.03
Dry hydrogel	500 ± 20	0.27 ± 0.07	0.07 ± 0.03

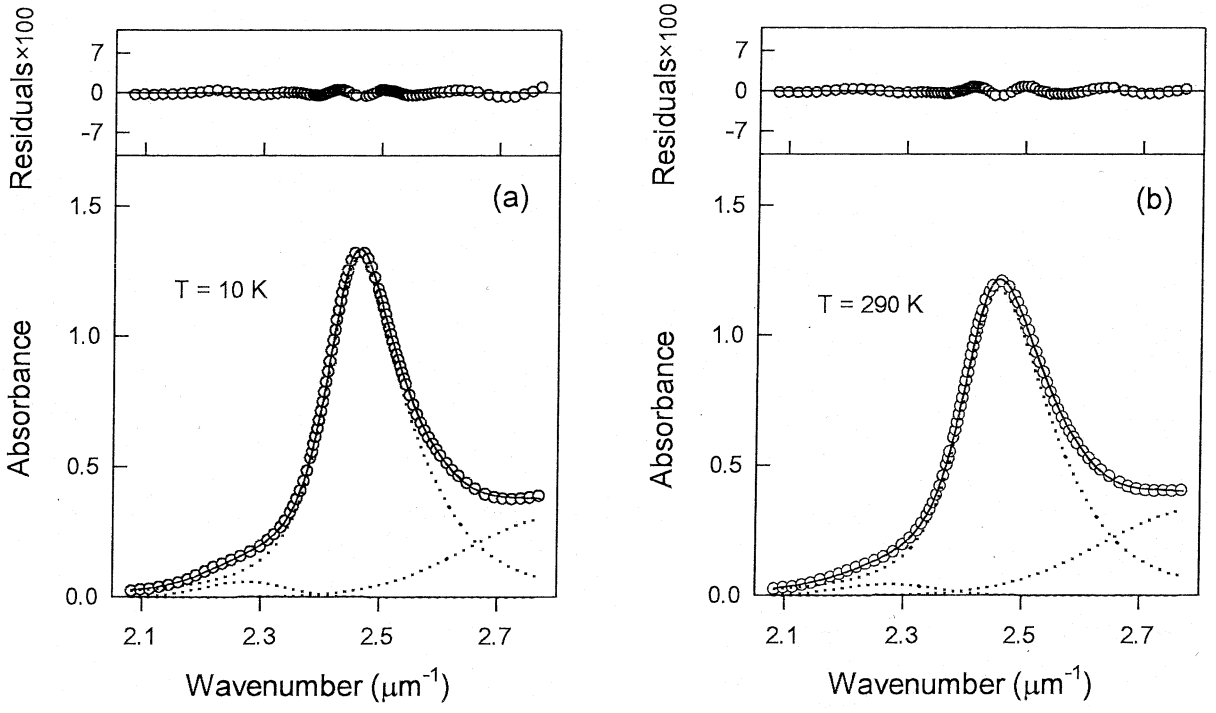

Fig. 3. Deconvolution of the Soret band of ferricytochrome *c* encapsulated within a 'dry' hydrogel at (a) 10 K and (b) 295 K. For the sake of clarity, not all the experimental points are reported. Dotted lines represent the spectral contribution of the main Soret band in terms of Eq. (1), of the N band (blue side region) and of the low-frequency band; the continuous lines represent the overall profiles synthesized. For each deconvolution, the residuals are also shown in the upper panels, on an expanded scale.

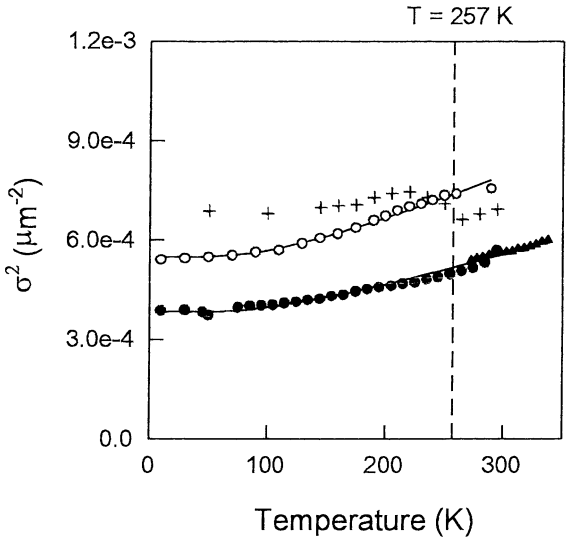

Fig. 4. Temperature dependence of parameter σ^2 for the wet hydrogel (crosses), dry hydrogel (open symbols), water and water/glycerol solutions (closed symbols). Continuous lines represent fittings in terms of Eq. (4).

very similar, the upward shift observed for the dry hydrogel data is essentially due to an increased value of parameter σ_{inh} i.e. of the inhomogeneous broadening. We attribute this effect to the interaction of the protein with the embedding silica matrix, which provides a more heterogeneous environment to the chromophore. However, protein–silica interactions are not such to alter substantially the active site dynamics of the encapsulated protein.

The thermal behavior of the 'wet' hydrogel is strikingly different. In fact, the σ^2 values show a decrease upon lowering the temperature only down to approximately 257 K. At temperatures between 265 and 250 K (i.e. when water in the 'wet' hydrogel freezes and the sample cracks, see Fig. 1) a sudden increase is observed, while, at lower temperatures, σ^2 values remain almost constant. This shows that the active site dynamics of ferricytochrome *c* is highly dependent upon the state of the solvent. In the 'wet' hydrogel freezing of the water introduces an increased local heterogeneity at the chromophore and, at the same time, quenches the bath of soft modes linearly coupled to the Soret band transition.

Table 2
Values of the parameters obtained by fitting the $\sigma^2(T)$ thermal behavior in terms of Eq. (4)

Conditions	$N{\cdot}S$	$\langle\nu\rangle$ (cm^{-1})	σ_{inh} (cm^{-1})
Solution	0.34 ± 0.06	225 ± 20	180 ± 8
Dry hydrogel	0.45 ± 0.06	225 ± 20	150 ± 7

Conversely, in the dry hydrogel, the system exhibits increased inhomogeneity—in view of the locally heterogeneous constraints imposed on the different proteins by the embedding silica matrix. However, since water is not frozen, and a percentage 'weakly bonded' water molecules is present even at 10 K (see Fig. 2 and Ref. [21]), the bath of soft modes linearly coupled to the Soret transition is not quenched, and the dynamic properties of the active site are very similar to those in solution.

The temperature dependence of the Soret band peak frequency (parameter ν_0) is reported in Fig. 5. The thermal behavior observed in the dry hydrogel is similar to the solution one, apart from an upward shift that can be attributed to a different local electric field experienced by the chromophore in the encapsulated protein. Surprisingly, no relevant effect is introduced in the thermal behavior

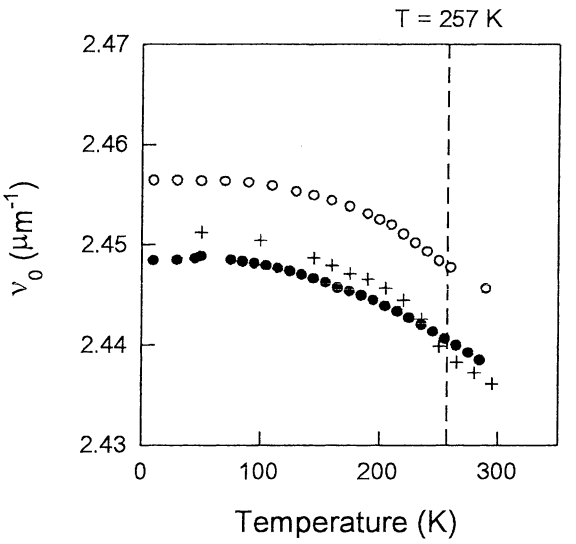

Fig. 5. Temperature dependence of parameter ν_0. Symbols as in Fig. 4.

of parameter ν_0 of the wet hydrogel by water freezing. To rationalize this observation, we recall that the temperature dependence of the peak frequency is brought about by vibrational modes quadratically coupled to the Soret band transition, while linearly coupled modes do not cause any peak frequency shift [18]. Data in Fig. 5, therefore, suggest that, for ferricytochrome *c*, the ensemble of modes quadratically coupled to the Soret transition is different from those linearly coupled, the former being almost independent on the interactions between water and the active site.

4. Conclusions

The main results obtained in this work may be summarized as follows:

(1) Use of an appropriate sol–gel protein encapsulation protocol enables to monitor, in the same sample, the dynamics of the protein active site (through the temperature dependence of the Soret band) and the structure of the solvent (through the temperature dependence of the NIR spectrum of water trapped in the hydrogel).

(2) Sol–gel encapsulation 'per se' introduces an increased heterogeneity in the active site of cytochrome *c* but does not alter its dynamic properties. This is clearly shown by the 'dry' hydrogel data in the whole temperature range and by the 'wet' hydrogel data at high temperatures ($T > 260$ K).

(3) The protein active site dynamics is highly dependent on the structure of water trapped in the hydrogel. In particular, freezing of the water in the wet hydrogel quenches the ensemble of soft modes linearly coupled to the Soret transition; conversely, in the dry hydrogel, water does not freeze, and an active site dynamics, similar to the non-freezing water/glycerol solution is observed. This behavior supports the suggestion, based on computer simulation and neutron scattering studies [30,31], of a strong interdependence of protein and hydration water dynamics.

Acknowledgments

We thank Mr G. Lapis of the cryogenic laboratory for technical help. This work has been supported by the COFIN 2000 funds from the Italian MIUR.

References

[1] L.M. Ellerby, C.R. Nishida, F. Nishida, et al., Encapsulation of proteins in transparent porous silicate glasses prepared by the sol–gel method, Science 255 (1992) 1113–1115.
[2] D. Avnir, S. Braun, O. Lev, M. Ottolenghi, Enzymes and other proteins entrapped in sol–gel materials, Chem. Mater. 6 (1994) 1605–1614.
[3] B.C. Dave, B. Dunn, J.S. Valentine, J.I. Zink, Sol–gel encapsulation method for biosensors, Anal. Chem. 66 (1994) 1120A–1127A.
[4] I. Savini, R. Santucci, A. Di Venere, et al., Catalytic and spectroscopic properties of cytochrome-*c*, horseradish peroxidase, and ascorbate oxidase embedded in a sol–gel silica matrix as a function of gelation time, Appl. Biochem. Biotechnol. 82 (1999) 227–241.
[5] E.H. Lan, B.C. Dave, J.M. Fukuto, B. Dunn, J.I. Zink, J.S. Valentine, Synthesis of sol–gel encapsulated heme proteins with chemical sensing properties, J. Chem. Mater. 9 (1999) 45–53.
[6] N. Shibayama, S. Saigo, Fixation of the quaternary structures of human adult hemoglobin by encapsulation in transparent porous silica gels, J. Mol. Biol. 251 (1995) 203–209.
[7] S. Bettati, A. Mozzarelli, T state hemoglobin binds oxygen noncooperatively with allosteric effects of protons, inositol hexaphosphate, and chloride, J. Biol. Chem. 272 (1997) 32050–32055.
[8] N. Shibayama, Kinetics of the allosteric transition in hemoglobin within silicate sol–gel, J. Am. Chem. Soc. 121 (1999) 444–445.
[9] I. Khan, C.F. Shannon, D. Dantsker, A.J. Friedman, J. Perez-Gonzalez-de-Apodaca, J.M. Friedman, Sol–gel trapping of functional intermediates of hemoglobin: geminate and bimolecular recombination studies, Biochemistry 39 (2000) 16099–16109.
[10] S. Bruno, M. Bonnaccio, S. Bettati, et al., High and low oxygen affinity conformations of T state hemoglobin, Protein Sci. 10 (2001) 2401–2407.
[11] U. Samuni, M.S. Navati, L.J. Juszczak, D. Dantsker, M. Yang, J.M. Friedman, Unfolding and refolding of sol–gel encapsulated carbonmonoxymyoglobin: an orchestrated spectroscopic study of intermediates and kinetics, J. Phys. Chem. B 104 (2000) 10802–10813.
[12] H. Frauenfelder, F. Parak, R.D. Young, Conformational substates in proteins, Ann. Rev. Biophys. Chem. 17 (1988) 451–479.
[13] P.J. Steinbach, A. Ansari, J. Berendzen, et al., Ligand binding to heme proteins: connection between dynamics and function, Biochemistry 30 (1991) 3988–4001.
[14] E.E. Di Iorio, U.R. Hiltpold, D. Filipovic, et al., Protein dynamics. Comparative investigation on heme-proteins

with different physiological roles, Biophys. J. 59 (1991) 742–754.
[15] C.E. Cameron, S.J. Benkovic, Evidence for a functional role of the dynamics of glycine-121 of *Escherichia coli* dihydrofolate reductase obtained from kinetic analysis of a site-directed mutant, Biochemistry 36 (1997) 15792–15800.
[16] M. Falconi, M.E. Stroppolo, P. Cioni, et al., Dynamics-function correlation in Cu, Zn superoxide dismutase: a spectroscopic and molecular dynamics simulation study, Biophys. J. 80 (2001) 2556–2567.
[17] A. Di Pace, A. Cupane, M. Leone, E. Vitrano, L. Cordone, Protein dynamics. Vibrational coupling, spectral broadening mechanisms, and anharmonicity effects in carbonmonoxy heme proteins studied by the temperature dependence of the Soret band lineshape, Biophys. J. 63 (1992) 475–484.
[18] A. Cupane, M. Leone, E. Vitrano, L. Cordone, Low temperature optical absorption spectroscopy: an approach to the study of stereodynamic properties of hemeproteins, 23 (1995) 385–398.
[19] B. Melchers, E.W. Knapp, F. Parak, L. Cordone, A. Cupane, M. Leone, Structural fluctuations of myoglobin from normal-modes, Mossbauer, Raman, and absorption spectroscopy, Biophys. J. 70 (1996) 2092–2099.
[20] V. Sanfratello, A. Boffi, A. Cupane, M. Leone, Heme symmetry, vibronic structure, and dynamics in heme proteins: ferrous nicotinate horse myoglobin and soybean leghemoglobin, Biopolymers (Biospectroscopy) 57 (2000) 291–305.
[21] A. Cupane, M. Levantino, M.G. Santangelo, Near infrared spectra of water confined in silica hydrogels in the temperature interval 365-5 K, J Phys Chem B, submitted for publication.
[22] V. Militello, M. Leone, A. Cupane, R. Santucci, A. Desideri, Local dynamic properties of the heme pocket native and solvent-induced molten-globule-like states of cytochrome *c*, Biophys Chem, in press.
[23] K.T. Schomacker, O. Bangcharoenpaurpong, P.M. Champion, Investigation of the Stokes and anti-Stokes resonance Raman scattering of cytochrome *c*, J. Chem. Phys. 80 (1984) 4701–4717.
[24] K.T. Schomacker, P.M. Champion, Investigations of spectral broadening mechanisms in biomolecules, J. Chem. Phys. 84 (1986) 5314–5325.
[25] C.K. Chan, J.B. Page, Temperature effects in the time correlator theory of resonance Raman scattering, J. Chem. Phys. 79 (1983) 5234–5250.
[26] C.K. Chan, J.B. Page, $T \neq 0$ multimode modeling of optical absorption spectra and resonance Raman profiles, Chem. Phys. Lett. 104 (1984) 1609–1614.
[27] C.A. Angell, V. Rodgers, Near infrared spectra and the disrupted network model of normal and supercooled water, J. Chem. Phys. 80 (1984) 6245–6252.
[28] H. Nishikawa, in: H.S. Nalwa (Ed.), Silicon-Based Materials and Devices, vol. 2, Academic Press, San Diego, 2001, pp. 93–122.
[29] V.H. Segtnan, T. Isaksson, Y. Ozaki, Studies on the structure of water using two-dimensional near-infrared correlation spectroscopy and principal component analysis, Anal. Chem. 73 (2001) 3153–3161.
[30] A.R. Bizzarri, A. Paciaroni, S. Cannistraro, Glasslike dynamical behavior of the plastocyanin hydration water, Phys. Rev. E 62 (2000) 3991–3999.
[31] A. Paciaroni, A.R. Bizzarri, S. Cannistraro, Neutron scattering evidence of a boson peak in protein hydration water, Phys. Rev. E 60 (1999) 2476–2479.